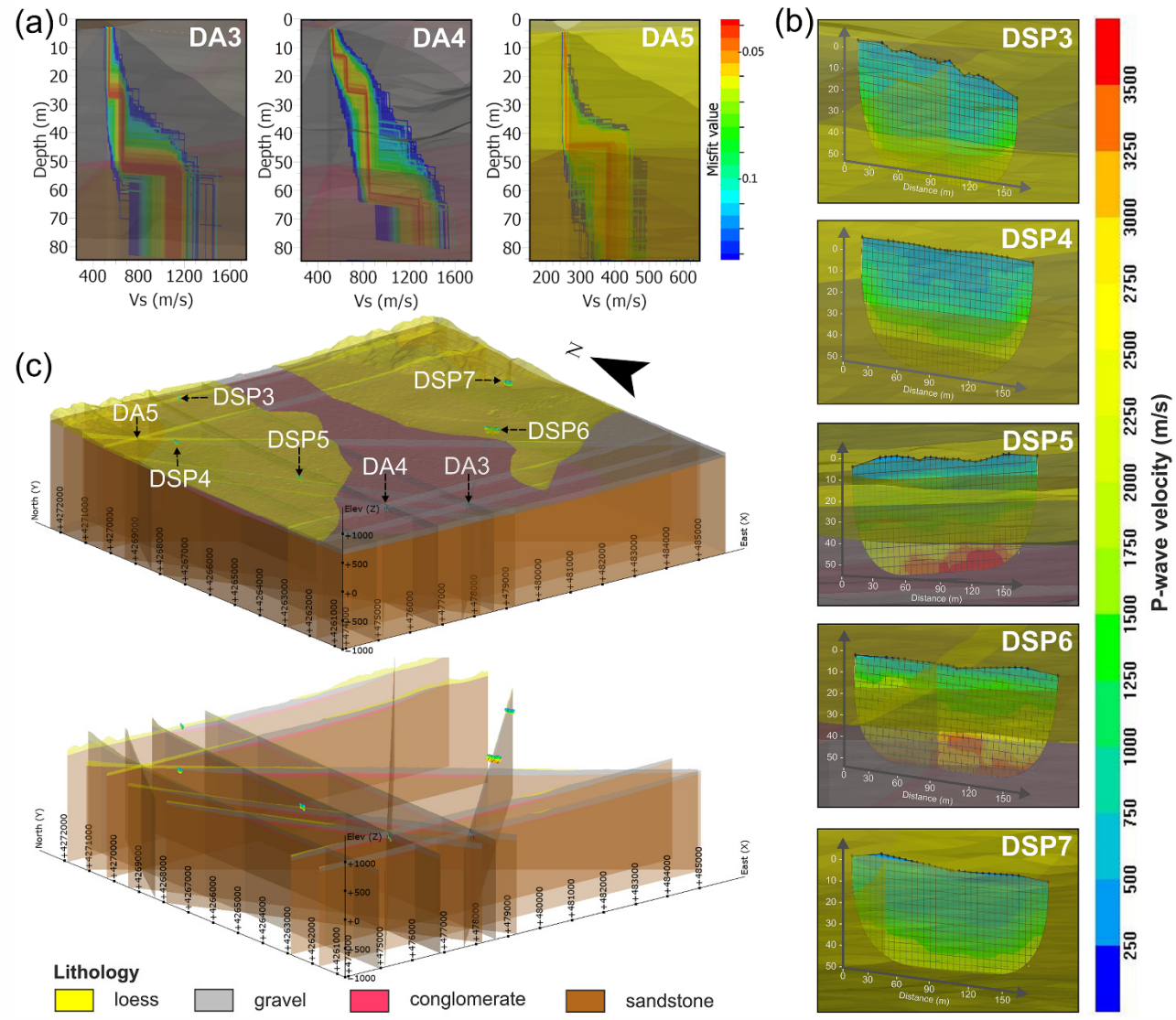

Figure S1. Integration of the 3D geomodel with results of microtremor array measurement (MAM) and seismic refraction tomography (SRT) geophysical measurements in the Dushanbe study area, based on the research by Hakimov et al. (2021); (a) Show microtremor array measurement (MAM) results for points DA3 (in the S), DA4 (in the SW), and DA5 (in the NW) with their projection onto the 3D geomodel; (b) Display of seismic refraction tomography (SRT) results for points DSP3 (in the NW), DSP4 (in the W), DSP5 (in the W), DSP6 (in the SE), and DSP7 (in the NE) with their visualization in the 3D geomodel; (c) Combined 3D geomodel demonstrating the results of MAM and SRT measurements, with surface models corresponding to the locations of geophysical measurements.

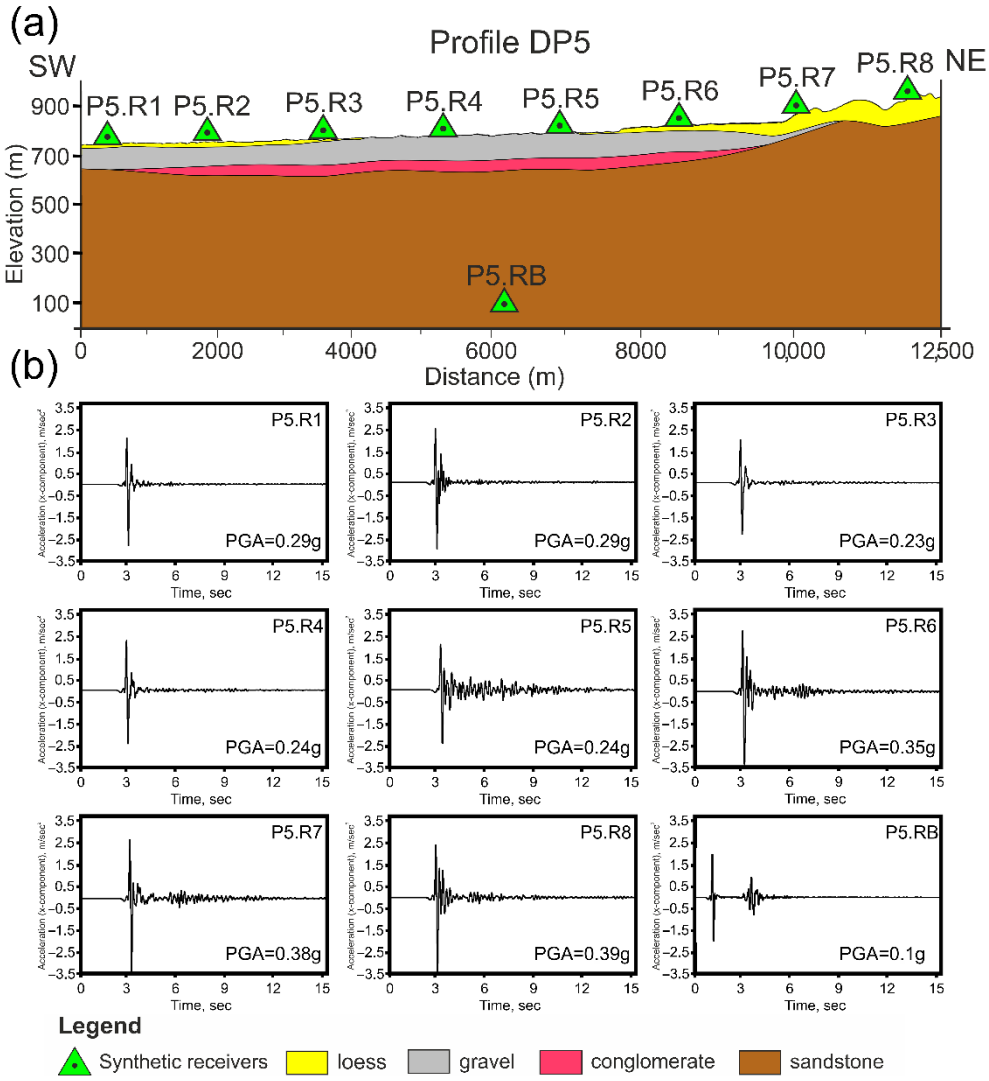

Figure S2. (a,b) Demonstration of PGA results for profile DP5. The graphs present acceleration data for the x-component, showing PGA (g) for eight surface receivers and one reference receiver.

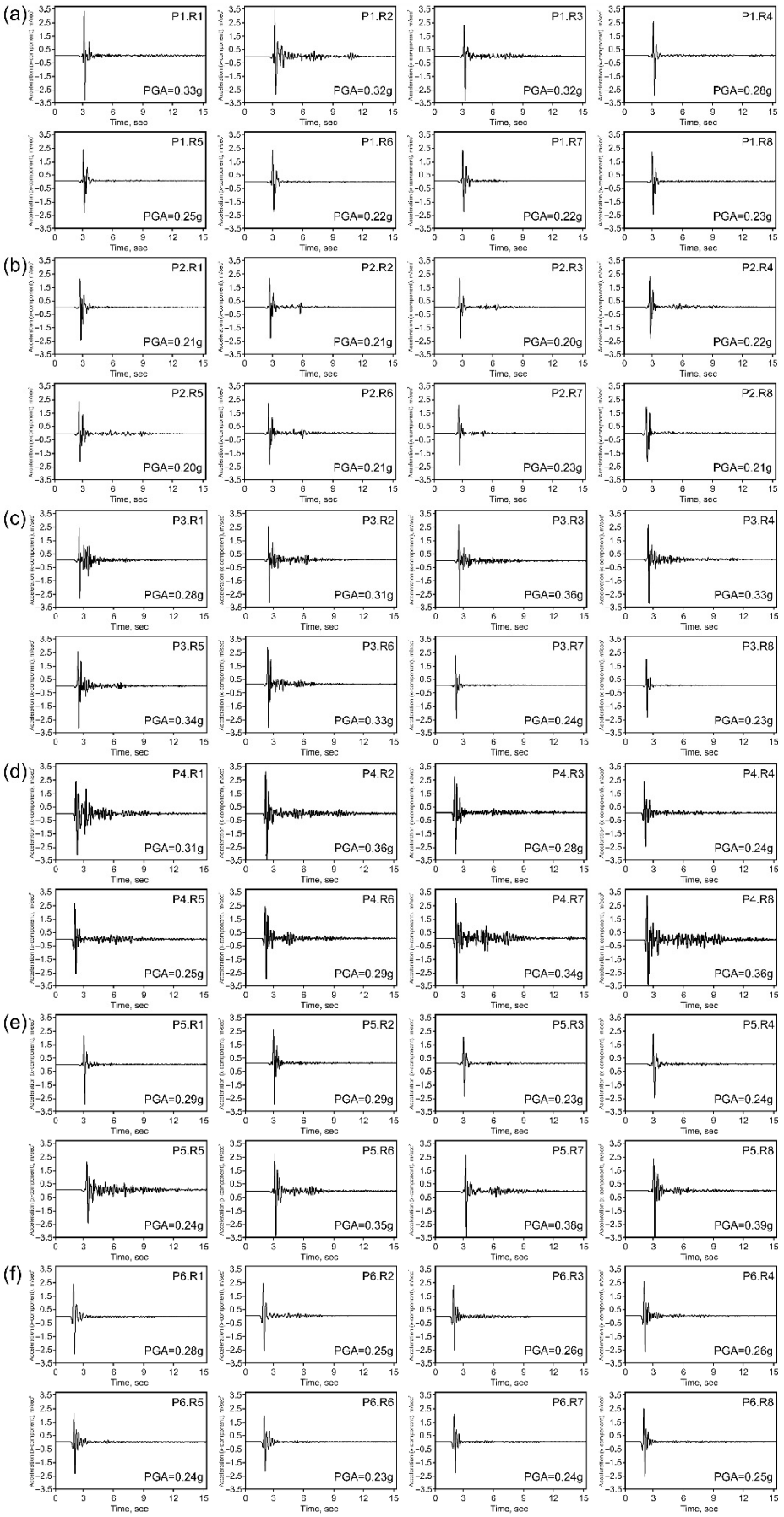
(a)
P1.R1 PGA=0.33g
P1.R2 PGA=0.32g
P1.R3 PGA=0.32g
P1.R4 PGA=0.28g
P1.R5 PGA=0.25g
P1.R6 PGA=0.22g
P1.R7 PGA=0.22g
P1.R8 PGA=0.23g
(b)
P2.R1 PGA=0.21g
P2.R2 PGA=0.21g
P2.R3 PGA=0.20g
P2.R4 PGA=0.22g
P2.R5 PGA=0.20g
P2.R6 PGA=0.21g
P2.R7 PGA=0.23g
P2.R8 PGA=0.21g
(c)
P3.R1 PGA=0.28g
P3.R2 PGA=0.31g
P3.R3 PGA=0.36g
P3.R4 PGA=0.33g
P3.R5 PGA=0.34g
P3.R6 PGA=0.33g
P3.R7 PGA=0.24g
P3.R8 PGA=0.23g
(d)
P4.R1 PGA=0.31g
P4.R2 PGA=0.36g
P4.R3 PGA=0.28g
P4.R4 PGA=0.24g
P4.R5 PGA=0.25g
P4.R6 PGA=0.29g
P4.R7 PGA=0.34g
P4.R8 PGA=0.36g
(e)
P5.R1 PGA=0.29g
P5.R2 PGA=0.29g
P5.R3 PGA=0.23g
P5.R4 PGA=0.24g
P5.R5 PGA=0.24g
P5.R6 PGA=0.35g
P5.R7 PGA=0.38g
P5.R8 PGA=0.39g
(f)
P6.R1 PGA=0.28g
P6.R2 PGA=0.25g
P6.R3 PGA=0.26g
P6.R4 PGA=0.26g
P6.R5 PGA=0.24g
P6.R6 PGA=0.23g
P6.R7 PGA=0.24g
P6.R8 PGA=0.25g
Time, sec

Figure S3. Acceleration time histories (x-component) and PGA values at selected surface receivers across six profiles in the study area: (a) Profile DP1 PGA results; (b) Profile DP2 PGA results; (c) Profile DP3 PGA results; (d) Profile DP4 PGA results; (e) Profile DP5 PGA results; (f) Profile DP6 PGA results.

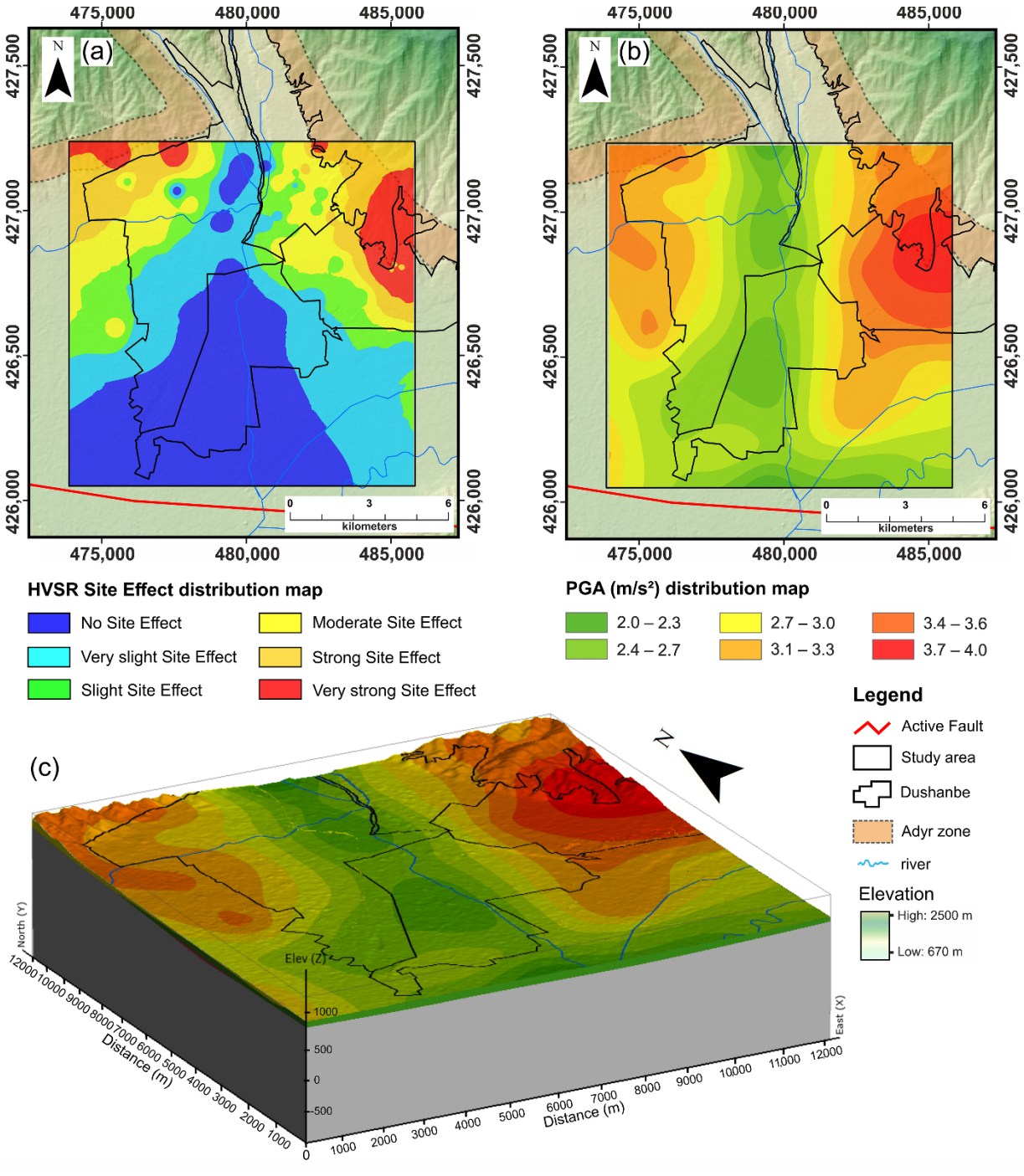

Figure S4. Analysis of the distribution of site effects and their comparison with the results of 2D dynamic numerical modeling in the study area. (a) Show the distribution of site effects, emphasizing the combined influence of the resonance frequency (f_0) and peak amplitude (A_0); (b) Show the distribution of PGA (m / s²) results, calculated using the Ricker wavelet for all surface receivers in the study area; (c) Visualization of the distribution of 2D dynamic numerical modeling results of PGA (m / s²) on a 3D model of the study area.